Atomistic mechanisms of rapid energy transport in light-harvesting molecules

Satoshi Ohmura,[1,3] Shiro Koga,[1] Ichiro Akai,[2] Fuyuki Shimojo,[1,3,b)] Rajiv K. Kalia,[3] Aiichiro Nakano,[3,a)] and Priya Vashishta[3]
[1]*Department of Physics, Kumamoto University, Kumamoto 860-8555, Japan*
[2]*Shock Wave and Condensed Matter Research Center, Kumamoto University, Kumamoto 860-8555, Japan*
[3]*Department of Computer Science, Department of Physics and Astronomy, Department of Chemical Engineering and Materials Science, Collaboratory for Advanced Computing and Simulations, University of Southern California, Los Angeles, California 90089-0242, USA*

(Received 29 December 2010; accepted 18 February 2011; published online 14 March 2011)

Synthetic supermolecules such as π-conjugated light-harvesting dendrimers efficiently harvest energy from sunlight, which is of significant importance for the global energy problem. Key to their success is rapid transport of electronic excitation energy from peripheral antennas to photochemical reaction cores, the atomistic mechanisms of which remains elusive. Here, quantum-mechanical molecular dynamics simulation incorporating nonadiabatic electronic transitions reveals the key molecular motion that significantly accelerates the energy transport based on the Dexter mechanism. © *2011 American Institute of Physics*. [doi:10.1063/1.3565962]

Harvesting energy from sunlight is of paramount importance for the solution of the global energy problem,[1] for which synthetic supermolecules such as light-harvesting dendrimers[2] are attracting great attention.[3] In these molecules, electronic excitation energy due to photoexcitation of antennas located on the periphery of the molecules is rapidly transported to the photochemical reaction centers at the cores of the molecules, which in turn perform useful work such as photosynthesis and molecular actuation.[4] A number of experimental[5–7] and theoretical[8] works have addressed rapid energy transport mechanisms in light-harvesting dendrimers. Though such energy transfer is conventionally attributed to either dipole–dipole interactions (Förster mechanism) or the overlapping of donor and acceptor electronic wave functions (Dexter mechanism),[2] atomistic mechanisms of rapid electron transport in these dendrimers remain elusive. Here, we perform quantum-mechanical (QM) molecular dynamics (MD) simulations incorporating nonadiabatic electronic processes[9,10] to identify atomistic mechanisms of rapid energy transport after photoexcitation of a light-harvesting dendrimer. The results reveal the key molecular motion (i.e., thermal vibration of the aromatic rings in the peripheral antennas), which significantly accelerates the energy transport based on the Dexter mechanism. The simulation results also elucidate the effect of temperature and solvent on the electron transport rate, which explains recent experimental observations.

The simulated system consists of a zinc-porphyrin core [labeled "core" in Fig. 1(a)] and a benzyl ether-type antenna. In the antenna, there are three aromatic rings connected by ether oxygen atoms, out of which one aromatic ring is directly connected to the zinc-porphyrin core. We hereafter refer to this ring as "intermediate" [labeled "inter" in Fig. 1(a)] and the other two rings bonded to the intermediate ring as "peripheries" [labeled "peri" in Fig. 1(a)]. The periodic boundary condition is employed with a suprecell of dimensions $18\times18\times24$ Å^3, which is large enough to avoid the interaction between periodic images of the molecule. Namely, the total energy changes only slightly ($\sim$0.01 meV/atom) when a larger supercell of $20\times20\times26$ Å^3 is used.

We first calculate the electronic structure of the system based on the density functional theory (DFT) (see Ref. 11 for the calculation method). The spatial distribution of some of the one-electron wave functions in the ground state is shown in Fig. 1(b), where the atomic positions are relaxed so as to minimize the total energy. It is seen from Fig. 1(b) that the highest occupied molecular orbital (HOMO) and the lowest unoccupied molecular orbital (LUMO) spread only within the core, which is consistent with the fact that electrons and holes photoexcited in the peripheries eventually move to the core. Figure 1(b) also shows the wave function of the occupied molecular orbital (MO) with the nth highest energy but

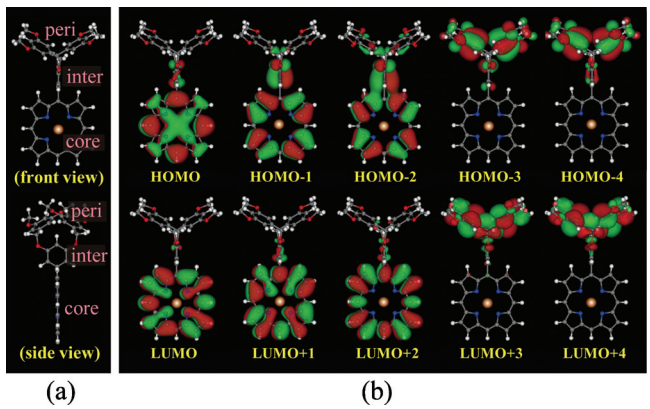

FIG. 1. (Color) (a) Simulated dendrimer consisting of a zinc-porphyrin core (labeled "core") and a benzyl ether-type antenna that has one "intermediate" (labeled "inter") and two "peripheries" (labeled "peri") rings. The brown, blue, gray, red, and white balls indicate Zn, N, C, O, and H atoms, respectively. (b) Spatial distribution of electronic wave functions in the ground state, for HOMO, HOMO$-n$ (MO with the nth lowest energy but one, $n=1-4$), LUMO, and LUMO$+m$ (MO with the mth highest energy but one, $m=1-4$), where red and green colors represent the isosurfaces of the wave functions with the values of 0.013 a.u. and -0.013 a.u., respectively.

a)Electronic mail: anakano@usc.edu.
b)Electronic mail: shimojo@kumamoto-u.ac.jp.

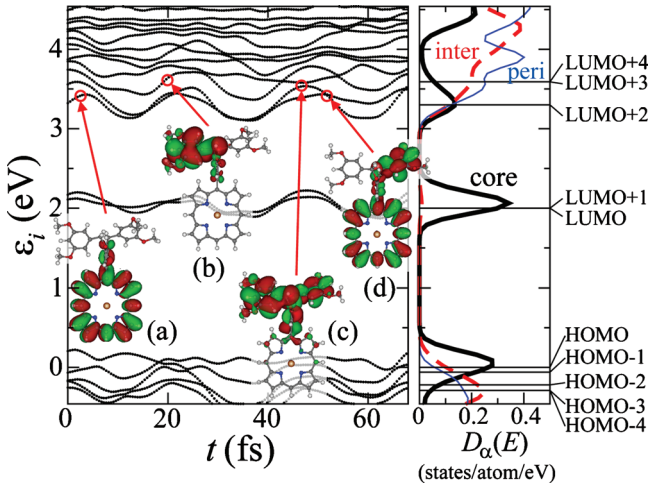

FIG. 2. (Color) (Left panel) Time evolution of electronic eigenenergies during adiabatic MD simulation for the ground state. Spatial distribution of an electronic wave function is also shown for (a) LUMO+2 at 3 fs, (b) LUMO+4 at 20 fs, (c) LUMO+3 at 47 fs, and (d) LUMO+2 at 52 fs. (Right panel) Time-averaged electronic DOS $D_\alpha(E)$, where the black solid, red dashed, and blue solid curves are for the core, intermediate, and peripheries, respectively.

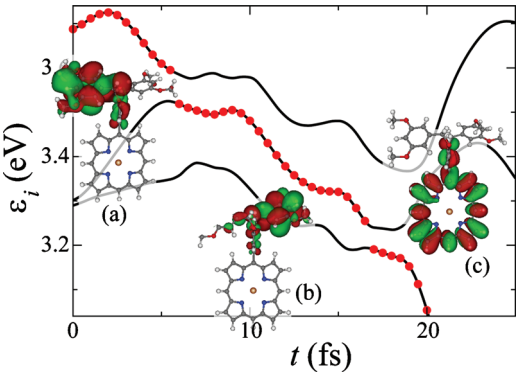

FIG. 3. (Color) Time evolution of electronic eigenenergies in TDKS-FSSH simulation. The red circles denote energies of the electronic states occupied by the photoexcited electron. The spatial distribution of the wave function of the photoexcited electron is also shown at time t=(a) 0, (b) 10, and (c) 20 fs.

one (denoted as HOMO−n, where n=1–4) and that of the unoccupied MO with the mth lowest energy but one (denoted as LUMO+m, where m=1–4). The wave functions of HOMO−1, HOMO−2, LUMO+1, and LUMO+2 are distributed mainly within the core. The eigenenergies of LUMO and LUMO+1 are almost degenerate within 0.01 eV, and they are separated well from the other states; the energy difference between HOMO and LUMO is about 2.0 eV, and that between LUMO+1 and LUMO+2 is about 1.3 eV. In contrast to these core states, HOMO−3, HOMO−4, LUMO+3, and LUMO+4 spread mainly within the peripheries.

To study the effect of thermal molecular motions on the electronic wave functions, we next perform adiabatic MD simulation at a temperature of T=300 K in the canonical ensemble, where the electrons stay in the ground state and the atomic forces are calculated based on the DFT.[12] The left panel of Fig. 2 shows the time evolution of electronic eigenenergies ε_i during the MD simulation. From the time average of these eigenenergies, we calculate electronic densities of states (DOS) $D_\alpha(E)$ projected to the wave functions of the atoms in molecular subsystems,[13] where α=core, inter, peri for the zinc-porphyrin core, intermediate ring, and peripheral rings, respectively. The right panel of Fig. 2 shows $D_{\text{core}}(E)$ (black solid curve), $D_{\text{inter}}(E)$ (red dashed curve), and $D_{\text{peri}}(E)$ (blue solid curve) at T=300 K, along with the eigenenergies of the optimized structure at T=0 K in Fig. 1 (horizontal lines). In $D_{\text{core}}(E)$, there are peaks at 0.1, 2.1, and 3.3 eV (the origin of energy is taken at the HOMO eigenenergy at 0 K), whereas $D_{\text{peri}}(E)$ has peaks at −0.3 eV and 4 eV. The differences between these energies are in good agreement with photoabsorption measurements at 25 °C;[14] the absorption peaks for the zinc-porphyrin core have been observed at the photon energies of about 2.2 and 3.0 eV (known as Q and Soret bands, respectively), and that for the peripheries has been observed around 4.4 eV.

Even at a finite temperature of 300 K, the two core states, LUMO and LUMO+1, are not mixed with the other states, represented by the clear distinct peak at ~2.1 eV in $D_{\text{core}}(E)$ (right panel in Fig. 2). In contrast, LUMO+2, which also spreads only within the core at 0 K, mixes with the states in the intermediate and peripheral rings due to thermal fluctuation at 300 K, and $D_{\text{core}}(E)$ above 3 eV overlaps with $D_{\text{inter}}(E)$ and $D_{\text{peri}}(E)$. The left panel of Fig. 2 exhibits multiple crossings of eigenenergies in this energy range. When an eigenenergy is well separated from the others, its wave function has a large amplitude only within the core or one of the peripheries as shown in Figs. 2(a) and 2(b), respectively. On the other hand, the wave function spreads over both peripheries, when the LUMO+3 and LUMO+4 energies approach each other [Fig. 2(c)]. Also, at a crossing of the LUMO+2 energy with another eigenenergy, the wave function spreads over both the core and a periphery [Fig. 2(d)]. This suggests that electrons photoexcited in the peripheries are transferred to the core through such extended state, i.e., by the Dexter mechanism. A similar situation is observed for the occupied states (HOMO, HOMO−1, …), which suggests that hole transport also occurs with the same mechanism.

In order to confirm that a photoexcited electron indeed transfers based on the Dexter mechanism, we perform nonadiabatic MD simulations that incorporate electronic transitions through the fewest-switches surface-hopping (FSSH) method[9] along with the Kohn–Sham (KS) representation of time-dependent (TD) DFT.[10] The nuclei are treated classically in the adiabatic representation, i.e., the atomic forces are calculated from the (excited) electronic eigenstates for the current nuclear positions. Switching probability from the current adiabatic state to another is computed from the density-matrix elements obtained by solving the TDKS equations,[10] and nonadiabatic transitions between adiabatic states occur stochastically.[9] We have estimated the many-body correction on an electron–hole pair excitation based on Casida's linear-response TDDFT (Ref. 15) and found that the switching probability is modified by at most a few percent (see Fig. S1, Ref. 11).

The TDKS-FSSH simulations are initiated by exciting an electron from the HOMO−4 to LUMO+4 state at time t=0, corresponding to the ultraviolet-light excitation in experiments.[14] We also calculate the distribution of oscillator strengths using Casida's linear-response TDDFT method,[15] which agrees well with the observed absorption spectra (see Figs. S2 and S3, Ref. 11). An example of the time evolution of the eigenenergies is shown in Fig. 3 (supplementary movie S1 shows this process, Ref. 11). Just after the excitation, the wave function of the occupied LUMO+4 is distrib-

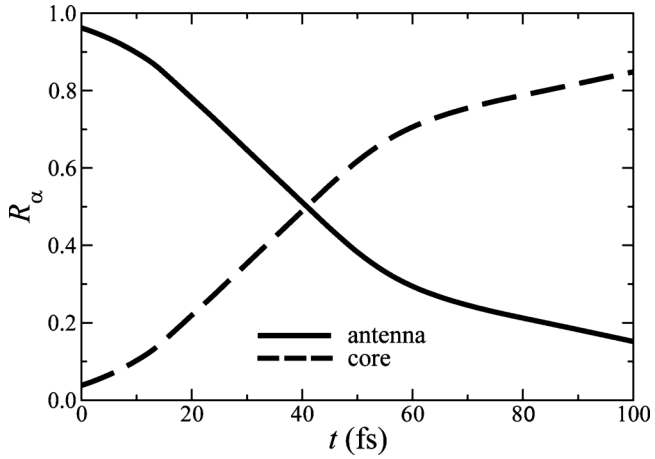

FIG. 4. Time evolution of the existence probability $R_\alpha(t)$ of a photoexcited electron. The solid and dashed lines indicate $R_\alpha(t)$ for the core and antenna regions, respectively.

uted mainly in the left periphery [Fig. 3(a)]. At 6 fs, a transition from LUMO+4 to LUMO+3 occurs, accompanied by the transfer of the electron to the right periphery [Fig. 3(b)]. Note that the eigenenergy of the right periphery is not always lower than that of the left periphery due to their crossings. At 17 fs, another transition to LUMO+2 occurs, causing the wave function of the occupied state to reside mainly within the core [Fig. 3(c)].

As demonstrated above, the crossings of eigenenergies ε_i due to thermal motions of atoms are crucial for electron transfer. With larger fluctuation of eigenenergies, the crossings are more frequent, resulting in fast energy transfer. The fluctuation of eigenenergies can be estimated from adiabatic MD simulations. We obtain the average standard deviation of eigenenergies $\sigma=\langle(\varepsilon_i-\bar{\varepsilon}_i)^2\rangle^{1/2}$, where $\bar{\varepsilon}_i$ is the time-averaged value and $\langle\cdots\rangle$ denotes the average over i=LUMO+2, LUMO+3, LUMO+4, as well as over time. From the time evolution of ε_i in Fig. 2, σ is calculated to be 0.13 eV at 300 K.[16] When the temperature is decreased to 100 K, our MD simulation exhibits much smaller fluctuation, σ=0.02 eV, which indicates that the energy transfer should be slower at lower temperatures (see Fig. S4, Ref. 11). This explains a recent experiment on light-harvesting dendrimers,[6] in which a remarkable temperature dependence of photoluminescence intensities indicates that the energy transfer from the peripheries to the core is suppressed at low temperatures (i.e., below 100 K).

Since photoluminescence experiments for dendrimers are carried out in a solvent,[6] we also consider the environmental effects on the electron transfer. We perform adiabatic MD simulations for the dendrimer molecule in anhydrous tetrahydrofuran, which is organic liquid consisting of $(CH_2)_4O$ molecules used in experiments.[7,14] We find that the solvent suppresses the thermal motion of atoms in the dendrimer (see Figs. S5 and S6, Ref. 11).

In order to estimate the electron transfer time, additional TDKS-FSSH simulations are carried out, and Fig. 4 shows the time evolution of the existence probability $R_\alpha(t)$ (α=core or antenna) of a photoexcited electron obtained from the ensemble average over 40 simulations (see also Fig. S7, Ref. 11). Here, the solid and dashed curves show $R_\alpha(t)$ for the core and antenna regions, respectively, which are calculated in the same way as $D_\alpha(E)$ (the antenna region is defined as the intermediate plus the peripheries). The electron transfer time is estimated to be ~40 fs. The corresponding electron transfer rate, 0.025 fs^{-1}, is found to be orders-of-magnitude larger than that due to the competing Förster mechanism (see Ref. 11).

In summary, our QM MD simulation incorporating nonadiabatic electronic transitions reveals the key molecular motion that significantly accelerates the energy transport based on the Dexter mechanism. An essential feature of the electronic structure to support the rapid electron transfer is the existence of unoccupied levels in the peripheries just above LUMO+2 of the core, and that of occupied levels in the peripheries just below HOMO of the core. Crossings of these energy levels occur due to thermal fluctuation even in the ground state. Upon photoexcitation, the motion of aromatic rings connected by ether bonds enhances the lowering of the energy of the photoexcited state, thereby promoting such crossings further. The acceleration is less pronounced in the presence of solvent at low temperatures which explains recent experimental observations.

This work was partially supported by DOE—EFRC/SciDAC-e and a Grant-in-Aid for JPSJ Fellows. S.O. and F.S. acknowledge support by Hamamatsu Photonics K.K., Japan.

[1]G. W. Crabtree and N. S. Lewis, Phys. Today **60**(3), 37 (2007).
[2]F. Vögtle, G. Richardt, and N. Werner, *Dendrimer Chemistry* (Wiley-VCH, Weinheim, 2009).
[3]B. L. Rupert, W. J. Mitchell, A. J. Ferguson, M. E. Kose, W. L. Rance, G. Rumbles, D. S. Ginley, S. E. Shaheen, and N. Kopidakis, J. Mater. Chem. **19**, 5311 (2009).
[4]T. Muraoka, K. Kinbara, and T. Aida, Nature (London) **440**, 512 (2006).
[5]I. Akai, H. Nakao, K. Kanemoto, T. Karasawa, H. Hashimoto, and M. Kimura, J. Lumin. **112**, 449 (2005).
[6]A. Yamada, A. Ishida, I. Akai, M. Kimura, I. Katayama, and J. Takeda, J. Lumin. **129**, 1898 (2009).
[7]I. Akai, K. Miyanari, T. Shimamoto, A. Fujii, H. Nakao, A. Okada, K. Kanemoto, T. Karasawa, H. Hashimoto, A. Ishida, A. Yamada, I. Katayama, J. Takeda, and M. Kimura, New J. Phys. **10**, 125024 (2008).
[8]Y. Kodama, S. Ishii, and K. Ohno, J. Phys.: Condens. Matter **21**, 064217 (2009).
[9]J. C. Tully, J. Chem. Phys. **93**, 1061 (1990).
[10]W. R. Duncan, C. F. Craig, and O. V. Prezhdo, J. Am. Chem. Soc. **129**, 8528 (2007).
[11]See supplementary material at http://dx.doi.org/10.1063/1.3565962 for simulation details.
[12]F. Shimojo, S. Ohmura, R. K. Kalia, A. Nakano, and P. Vashishta, Phys. Rev. Lett. **104**, 126102 (2010).
[13]F. Shimojo, A. Nakano, R. K. Kalia, and P. Vashishta, Phys. Rev. E **77**, 066103 (2008).
[14]I. Akai, T. Kato, K. Kanemoto, T. Karasawa, M. Ohashi, S. Shinoda, and H. Tsokube, Phys. Status Solidi C **3**, 3420 (2006).
[15]M. E. Casida, in *Recent Advances in Density Functional Methods (Part I)*, edited by D. P. Chong (World Scientific, Singapore, 1995), p. 155.
[16]We have confirmed that extra benzenes attached to the zinc-porphyrin core, as in the experiments (Ref. 14), have almost no effects on the fluctuation of eigenenergies.